Effect of elastic interactions on coarsening in elastically inhomogeneous multiphase systems

Danny Perez* and Laurent J. Lewis†

Département de Physique et Regroupement Québécois sur les Matériaux de Pointe (RQMP), Université de Montréal, Case Postale 6128, Succursale Centre-Ville, Montréal (Québec), Canada H3C 3J7

(Received 3 October 2006; published 3 April 2007)

We investigate the effect of interactions between inclusions on the coarsening behavior of elastically inhomogeneous multiphase systems with lattice misfit using a recently introduced two-dimensional multiscale model based on the classical time-dependent density-functional theory. We show that spontaneous shape changes are very efficient in limiting the impact of the interactions on the chemical potential of inclusions. For this reason, the interactions between isolated pairs of inclusions are unable to significantly affect coarsening. At higher volume fraction, the efficiency of shape changes drops and major shifts of the chemical potential are observed; these are shown to be strong enough to counteract capillarity. For example, we show that sufficient confinement by neighboring inclusions causes inverse coarsening and we provide illustrations of this. We also examine the effect of interface elasticity in the presence of interactions. We demonstrate that elasticity induces kinetic faceting and gives rise to oscillations in the chemical potential of the inclusions. This is shown to lead to the stabilization of microstructures composed of inclusions of various sizes. Finally, we propose a simple modified Lifshitz-Slyozov-Wagner model for assessing the effect of interactions on coarsening. The results are shown to be in excellent agreement with experiment.

DOI: 10.1103/PhysRevE.75.041602 PACS number(s): 81.10.−h, 61.66.Dk, 61.72.Qq, 64.75.+g

I. INTRODUCTION

It is well known that the macroscopic properties of materials depend strongly on their chemical composition. It is perhaps less appreciated that their macroscale behavior is also directly related to the microstructure. Indeed, nearly all properties of materials—optical [1,2], electrical [3], and, of course, mechanical [4,5]—are affected by micro- and even mesoscale morphological features. Control over the microstructure is thus essential to exploiting the full potential of materials. However, over sufficiently long periods of time, microstructural evolution may lead to the degradation of the performance of materials, a phenomenon known as aging. Reliable models of microstructural evolution are thus required in order to fully optimize materials with respect to specific applications.

The canonical model for microstructural evolution ("coarsening") in multiphase systems is that of Lifshitz and Slyozov [6] and Wagner [7] (LSW). It describes the evolution of a collection of spherical domains interacting diffusively under the following assumptions: (i) the capillarity approximation is valid; (ii) the dynamics is exclusively capillarity driven; and (iii) the density of inclusions is vanishingly small (dilute limit). Within the limits of these assumptions, it was shown that coarsening proceeds through the growth of large inclusions at the expense of small ones so that the average size of the inclusions $\langle R \rangle$ increases as $t^{1/3}$ (in the diffusion-limited regime). This behavior—also known as Ostwald ripening [8] or normal coarsening—has been observed in a wide range of phases, materials, and geometries. It eventually leads to complete phase separation with only one domain remaining; from a technological perspective, this is a rather unpleasant state of affairs.

Fortunately, it is known that microstructures do not always evolve according to the LSW theory. The possibility of controlling microstructural evolution opens the door to a wealth of interesting applications; stabilizing the microstructure is itself of great importance as it could help extend the lifetime of materials, perhaps considerably. In the present investigation, we are concerned with a particular class of materials exhibiting abnormal microstructural evolution, viz., elastically inhomogeneous multiphase alloys with lattice misfits, where the microstructure is composed of inclusions (or precipitates) of a given material embedded within a matrix made out of a different material. A multiphase alloy is said to be elastically inhomogeneous if the elastic constants of the matrix and the inclusions are different. Since such microstructure naturally forms from supersaturated solid solutions, multiphase alloys are commonplace in materials science.

The kinetics of microstructural evolution is known to be strongly affected by elastic effects. Slowdown relative to the LSW behavior, or even complete stabilization, has been reported in such materials as Ni-Cu-Si [9], Ti-Mo [10], Ni-Al-Ti [11], Ni-Al-Mo [12], etc. In some cases, slowing down is preceded by a normal coarsening phase [9–11]. Variations of the coarsening exponent or of the asymptotic average inclusion size as a function of the volume fraction of inclusions have been frequently reported [9,13]. Also, the morphology of the microstructures exhibits features that are not explained by the standard theory. For example, elasticity is known to induce shape transition in inclusions [12,14] as well as spatial correlations in both shape and position [11,12,15]; further, the size distribution is strongly affected as both widening [11,12,16] and narrowing [13] have been reported. It is generally accepted that these deviations from the LSW behavior stem from the fact that the relaxation of

*Present address: Theoretical Division T-12, Los Alamos National Laboratory, MS B-268, Los Alamos, NM 87545, USA.

†Author to whom correspondence should be addressed. Email address: Laurent.Lewis@UMontreal.CA

the elastic energy (originating from either inclusion-matrix or inclusion-inclusion interactions) competes with the decrease of the interfacial energy, hence violating assumption (ii) of the model. While the nature of the root cause is identified, the mechanisms leading to such strong changes in kinetics are still subject to debate. It should be noted that in real systems the elastic constants are often anisotropic in addition to being inhomogeneous. While anisotropy influences strongly the morphology of the microstructure, it is now well established—both theoretically [17] and experimentally [9]—that its effect on coarsening is small compared to that of the inhomogeneities. We thus focus on inhomogeneous, but isotropic, systems in the present study.

The objectives of the present work are threefold. First, we reconsider the problem of interacting inclusions using a two-dimensional multiscale model we introduced recently [18]. As is typical for such investigations [19–23], we describe the changes in the morphology of the inclusions arising from interactions but, in contrast with most of the above references (see Ref. [24] for a notable exception), we are mainly concerned with modifications to the thermodynamic force that drives coarsening, as obtained by measuring the chemical potential shifts induced by elastic interactions in either two-inclusion systems or periodic arrays of inclusions. We show that, in two-inclusion systems, spontaneous shape changes are extremely efficient in attenuating the effects of interactions, leading to small chemical potential shifts even at very short range. If, however, the inclusions are organized in a periodic fashion, thus reducing the efficiency of shape changes, very large shifts—proportional to the volume fraction of inclusions—are measured. We demonstrate that these elastic corrections are sufficient to significantly alter the coarsening behavior. Second, following up on our previous work [25,26], we examine a problem that has been largely overlooked, namely, the effect of interface elasticity on the coarsening behavior of systems of interacting inclusions. We show that high interface elastic misfits increase the efficiency of kinetic faceting, hence modifying the behavior of inclusions during growth. The misfits also induce oscillations in the chemical potentials; these oscillation are able to stabilize systems of inclusions of different sizes, even in presence of elastic interactions. A stable system of two inclusions is presented to illustrate this point. Third, and finally, using the results of the simulations, we propose a modified LSW model for the effect of elasticity on coarsening. The model is able to reproduce the essential characteristics of the experimental observations mentioned above. Based on these results, we propose that widening of the distribution of inclusions is related to strong interface misfits while narrowing is a consequence of inverse coarsening. We also show that inverse coarsening occurs in simple systems if the confining effect of the environment is taken into account. Finally, we show that our model is able to account for the wide variety of coarsening anomalies described above.

II. THEORETICAL BACKGROUND

From a theoretical point of view, the study of interactions in elastically inhomogeneous systems dates back to Eshelby [27], who first obtained an expression for the interaction energy between two spherical inclusions with radii R_1 and R_2, respectively, embedded in a matrix and separated by a distance D:

$$E_{\text{int}} = \frac{8\pi}{81}\left(\frac{1+\nu}{1-\nu}\right)^2 [q]^2[G]\left(\frac{R_1^6 R_2^3}{(D^2-R_2^2)^3} + \frac{R_2^6 R_1^3}{(D^2-R_1^2)^3}\right), \tag{1}$$

where ν is the Poisson ratio, $[q]$ is the lattice misfit between the two phases, and $[G]$ is the difference in shear moduli between the inclusions and the matrix. This equation is valid to first order in $[G]$, and thus for small inhomogeneities. Eshelby's formula has frequently been employed to discuss the effect of interactions on both the morphology and the kinetics of inhomogeneous systems. For example, concerning the morphology, the interactions are predicted to be repulsive or attractive for hard or soft inclusions, respectively, and should thus lead to positional correlations between inclusions [28,29], in agreement with experimental observations. The formula also suggests that coarsening kinetics would be strongly affected by elasticity. For example, for a fixed total inclusion volume, E_{int} is minimal for $R_1=R_2$ if the inclusions are soft ($[G]<0$). The interaction energy is thus expected to counteract the normal capillarity-driven tendency for the larger inclusion to grow at the expense of the smaller one, giving rise to inverse coarsening where the small inclusion grows until it reaches the size of the large one [30]. In contrast, for hard inclusions, the interaction energy is minimum when the size of the small inclusion vanishes. In this case, elastic interactions promote coarsening. In fact, it was shown by Enomoto and Kawasaki [31]—also assuming spherical inclusions—that for soft inclusions, the average inclusion size initially increases as $t^{1/3}$, but later completely stops because of inverse coarsening; for hard inclusions, the normal regime is followed by an acceleration of coarsening with $\langle R\rangle \propto t^{1/2}$. These authors have also predicted a narrowing (widening) of the size distribution function for soft (hard) inclusions.

While of appealing simplicity, a description of coarsening based on Eshelby's formula is unable to account for the wide variety of behaviors observed. For example, slowing down has been reported in systems of hard inclusions as well [9]. Also, widening of the distribution function can occur concomitantly with slowing down [11,12]. Such disagreements between theory and experiment may stem from two causes. First, energetics alone is not sufficient to determine the dynamics of systems driven by diffusion since the existence of an energy minimum does not ensure that it can be reached dynamically. Second, the validity of Eshelby's formula [Eq. (1)] is not always guaranteed: strictly speaking, it is correct only for spherical inclusions while it is known that elastic interactions strongly affect the shape of inclusions. In fact, it was demonstrated by Onuki and Nishimori [32] that two interacting circular inclusions adjust their shapes such as to cancel the anisotropic components of the strain field. This process was shown to be very efficient in reducing the interaction energy; the effect of interactions on coarsening is thus probably much lower than could have been expected from

Eshelby's formula. The robustness of inverse coarsening as a possible pathway to stabilization is hence also questioned.

The relevance of this observation was confirmed in subsequent simulations where constraints on the shape of the inclusions were lifted. For homogeneous but anisotropic elasticity, simulations of microstructures composed of a few inclusions showed that, while transient inverse coarsening is common, it does not persist long enough to lead to complete stabilization of the structure [33]. For elastically inhomogeneous systems, however, a two-inclusion configuration can minimize the energy [21], suggesting that stabilization through inverse coarsening can indeed occur. However, under diffusive dynamics, complete stabilization was not observed except for highly symmetric initial conditions [34].

In spite of these observations, the stabilization of complex microstructures was reported by Onuki and Nishimori [23]. Their simulations showed an initial, normal coarsening stage, followed by a transition to a frozen state, suggesting that stabilization does not necessarily involve inverse coarsening and that it might in fact be a very robust process occurring even in complex geometries. Concerns about the validity of these results were, however, raised by Chen and collaborators who, using an improved formalism for the calculation of the elastic energy [35], did not observe stabilization but, instead, a gradual (and rather slow) decrease of the coarsening exponent, from 1/3 in homogeneous systems to about 1/4 for a threefold difference in shear moduli between the two phases [22]. Other large-scale simulations also showed important reductions of the coarsening rate, but the effect on the coarsening exponents could not be inferred precisely [36].

The origin of the transition from normal coarsening to a stable (or slowly evolving) state observed in experiment [9–13] is thus still subject to debate. Further, the role of inverse coarsening in the anomalous behavior of elastically inhomogeneous systems remains unclear since it is seldom observed in simulations. However, as mentioned earlier, some alloys show a narrowing of the size distribution in the slow regime, strongly suggesting that inverse coarsening does occur in certain conditions. Finally, it remains to be understood why slowing down of coarsening is sometimes associated with narrowing of the size distribution function, and sometimes with widening.

III. MODEL AND COMPUTATIONAL DETAILS

As mentioned earlier, we are interested in both bulk and interface elastic contributions. A proper treatment of these requires an atomic-scale description of the interphase boundaries. In the present investigation, this is achieved using a multiscale model we recently proposed [18], which is based on the time-dependent density-functional theory (TDDFT) for classical lattice systems developed by Reinel, Fischer and collaborators [37–39]. The TDDFT provides a system of master equations for the evolution of the occupation probabilities of each site on the lattice. In our particular implementation, the TDDFT equations are solved using a multiscale framework where the resolution of the calculation varies from fully resolved at the atomic scale near interphase boundaries to coarse grained within the bulk phases. This enables us to treat large systems at a reasonable computational cost. Further, our implementation also includes the effect of elasticity using the quasicontinuum method of Tadmor and collaborators [40,41]. Note that our treatment of elasticity imposes coherency at the interface between inclusion and matrix, so that plasticity effects are not taken into account. This restricts our simulations to modest misfits. Also note that local elastic relaxation effects are treated at the mean-field level. A complete description of the model can be found in Ref. [18], and an outline is given in Ref. [26]. As will be shown below, our method has the unique advantage of giving access to thermodynamical quantities (e.g., chemical potentials), a feature usually associated with mesoscale phase-field models, while preserving the atomistic, Monte Carlo–like description of the microstructure as required.

TABLE I. Values of the stiffnesses k_{XY} and lattice constants σ_{XY} for the various types of inclusions considered in the present work. Stiffnesses are in units of ϵ/σ^2 and lattice constants in units of σ.

Type	k_{AA}	k_{AB}	k_{BB}	σ_{AA}	σ_{AB}	σ_{BB}
HI-LM	50	50	150	1.00	1.03	1.03
HI-HM	50	50	150	1.00	1.00	1.03
SI-LM	50	50	10	1.00	1.00	1.03
SI-HM	50	50	10	1.00	1.03	1.03

In this work, we consider a two-dimensional binary alloy with vacancies (ABv) and use the TDDFT to model the evolution in time of inclusions composed of a B-rich phase embedded within an A-rich matrix. The atoms are assumed to interact with their first neighbors through a harmonic potential of the form

$$V_{i,j}^{\alpha,\beta} = k^{\alpha,\beta}(r_{i,j} - \sigma^{\alpha,\beta})^2 - \epsilon^{\alpha,\beta}, \tag{2}$$

where $r_{i,j}=|\vec{r}_i-\vec{r}_j|$; i,j refer to lattice sites and α,β to atomic species. The underlying lattice is triangular. All results will be expressed in dimensionless, reduced units relative to a stress-free pure A phase: lattice parameter for length (σ), interaction energy between nearest neighbors for energy (ϵ), and inverse trial frequency (τ_0) for time. In all cases, the temperature is $T=0.5\epsilon/k_B$ (about half of the critical temperature for phase separation) and the vacancy concentration is 10^{-3}.

The bulk lattice misfit between the two phases is fixed to 3%. Four different combinations of elastic stiffnesses and lattice parameters are considered, as listed in Table I, namely, hard inclusions with low interface misfit (HI-LM), hard inclusions with high interface misfit (HI-HM), soft inclusions with low interface misfit (SI-LM), and soft inclusions with high interface misfit (SI-HM). An inclusion is hard (soft) if $k_{BB}>(<)k_{AA}$. The interface misfit qualifies the difference between σ_{AB} and the typical lattice constant near the interfaces. Since a hard inclusion tends to impose its lattice constant on nearby matrix material, a low interface misfit corresponds to $\sigma_{AB}=\sigma_{BB}$ while a high interface misfit corresponds to $\sigma_{AB}=\sigma_{AA}$. For soft inclusions, the opposite is true. Other param-

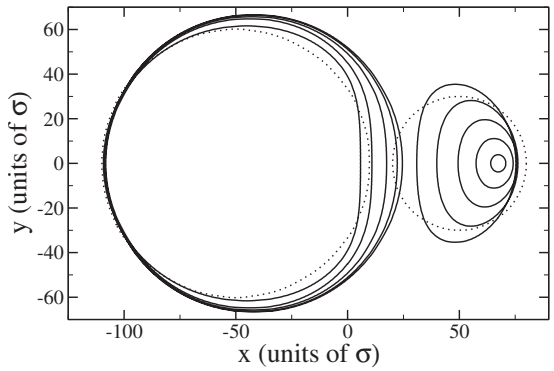

FIG. 1. Evolution in time of two HI-LM initially separated by $D=100\sigma$ during coarsening. The dotted line represents the initial configuration.

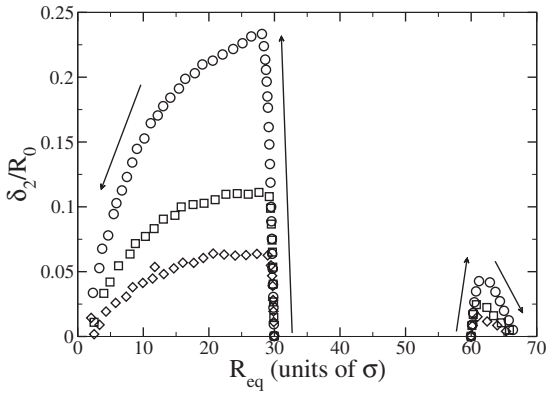

FIG. 2. Relative amplitude of mode 2 for different distances D between two HI-LM with initial radii of 30σ and 60σ, respectively: circles, $D=100\sigma$ (cf. Fig. 1); squares, $D=150\sigma$; diamonds, $D=200\sigma$. Arrows indicate the flow of time.

eters of the potential are $\epsilon_{AA}=\epsilon_{BB}=\epsilon$, $\epsilon_{AB}=0.7\epsilon$. While typical of real alloys, the model parameters are somewhat arbitrary and will likely affect the regimes in which either interfacial or elastic effects dominate; however, the physics of the microstructural evolution is not expected to be qualitatively affected by the precise value of these parameters.

The present study is based on two main types of simulations. First, we consider systems of two initially circular inclusions of radii $R=60\sigma$ and 30σ, respectively. In this case, calculations are carried out within an hexagonal cell of side 1536σ with closed boundary conditions (no flux in or out of the cell) for the TDDFT (diffusion) equations, and zero-displacement boundary conditions for the elastic equilibrium equations. Such a large cell size is required to eliminate finite-size effects. Second, we consider periodic arrays of inclusions. The simulation cell in this case is a parallelogram with a single inclusion placed at its center. Interactions between inclusions are introduced through periodic boundary conditions on the elastic equilibrium equation. When needed, growth is activated by imposing a constant chemical potential along the edge of an hexagon centered on the inclusion. Using this technique, all inclusions of the periodic array grow simultaneously.

IV. RESULTS

In order to isolate the effects of bulk elasticity from those related to interfaces, we examine first the case of hard inclusions with low misfit (HI-LM), then move on to study soft inclusions with low misfit (SI-LM); the peculiar behavior arising from large interface misfits will be discussed in Sec. IV C.

A. Interaction between hard inclusions

1. Two-inclusion systems

We consider first a system of two inclusions placed at the center of a very large cell. An example of the evolution of such a system is presented in Fig. 1. As soon as time starts running, the "inner" surfaces (between the two inclusions) strongly repel each other, leading to an elongation in the direction perpendicular to the axis joining the two inclusions. Such conformational changes have been predicted by Johnson *et al.* [42] and subsequently observed in numerous simulations [43,44]. They can in fact be expected on the basis of Eshelby's formula since the interaction energy between two HI is repulsive. As mentioned earlier, it was shown by Onuki and Nishimori [32] that shape changes occur so as to cancel the anisotropic components of the strain field within the inclusions. Note however that the inclusions as a whole do not move away from each other (the outer edges do not move during the simulation; see Fig. 1), as observed when a circular shape is imposed [28,45].

Morphological modifications can be quantified using a normal-mode analysis where the angular dependence of the radii of the inclusions is decomposed into a sum of cosines, viz., $R(\theta)=R_0+\Sigma_l \delta_l \cos(l\theta+\phi_l)$. In the present case, the leading contribution comes from mode $l=2$ since this corresponds to a uniaxial elongation. Figure 2 clearly shows the rapid development of the elongated shape, particularly so for the small inclusion ($R\leq 30$) where the modulation reaches about 25% of the radius (R_0) at small interinclusion distance D, compared to roughly 5% for the large inclusion ($R\geq 60$).

These shape changes do not occur following the condensation or evaporation of solute atoms, as the sizes of the inclusions are approximately constant until maximum deformation is reached (see Fig. 2). At this point, however, solute atoms start to diffuse from the small inclusion toward the large one, i.e., coarsening begins; we note that inverse coarsening was never observed in such configurations, even for smaller differences in the size of the two inclusions. Growth and evaporation are strongly anisotropic: the exchange of mass occurs almost exclusively at the inner surfaces, leaving the outer ones practically unaffected. As coarsening proceeds, the inclusions become increasingly circular ($\delta_2 \rightarrow 0$)—the large one because the strain field of the small one gradually gets weaker compared to its own, and the small one because of the increasing importance of capillarity (which favors a circular shape) as size decreases. The anisotropic character of the flow of solute atoms also favors the gradual return of the large inclusion to its equilibrium shape.

While the amplitude of the shape changes gives an indication of the strength of elastic interactions, it cannot be used

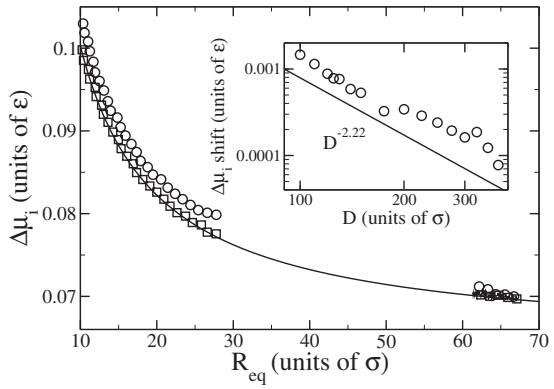

FIG. 3. Chemical potential difference $\Delta\mu_i$ between species B and species A as a function of size for two HI-LM with initial radii of 30σ and 60σ, respectively: circles, $D=100\sigma$; squares, $D=300\sigma$; continuous line, $\Delta\mu_i$ for an isolated inclusion. Inset: shift in $\Delta\mu_i$ in the small inclusion as a function of D.

directly to predict the effect on coarsening. Indeed, large variations in the shape imply extensive relaxation in response to an initially strong interaction, but the interactions are not necessarily strong once relaxation is completed. To obtain information about coarsening, one must measure changes in the thermodynamic force which drives diffusion, given here by the difference in chemical potentials $\Delta\mu_i^1 - \Delta\mu_i^2$, with $\Delta\mu_i^k = \mu_B - \mu_A$ within inclusion k. The evolution of $\Delta\mu_i$ for each of the two inclusions is presented in Fig. 3 for two different separations D; for reference, $\Delta\mu_i$ for an isolated inclusion (continuous line; fit to the data of Ref. [26]) is also plotted. As expected, when the distance between the inclusions is large (e.g., $D=300\sigma$), the interactions do not significantly affect $\Delta\mu_i$ and the two inclusions behave as if they were isolated; in this case, elasticity evidently does not affect the coarsening behavior of the system in any significant manner. However, as the distance decreases, the repulsive character of the interactions manifests itself, essentially through an upward shift of $\Delta\mu_i$; note that the shift mostly concerns the small inclusion ($R \leq 30$), leaving the large one ($R \geq 60$) almost unaffected. This anisotropy results in an increased driving force for coarsening ($\Delta\mu_i^1 - \Delta\mu_i^2$ increases) and hence accelerated coarsening compared to the elastically homogeneous case. The magnitude of the shift is, however, relatively small compared to the variations due to size changes, even at very small D. Further, as shown in the inset to Fig. 3, the shift (as obtained by fitting the different $\Delta\mu_i$ curves to a smooth function of $1/R_{eq}$) decreases rapidly with increasing distance ($\sim D^{-2.22}$). This points to the high efficiency of shape changes in lowering the interaction energy, and therefore minimizing the effect on coarsening.

2. Periodic arrays of inclusions

If shape changes are efficient in limiting the impact of pair interactions on coarsening, the behavior of microstructures containing a large density (volume fraction) of inclusions cannot be inferred from the study of simple configurations composed of only a few inclusions. In denser arrangements, the efficiency of the relaxation process is likely to decrease sharply because of the more stringent constraints imposed by many-body effects. Since a direct simulation of large multi-inclusion systems would be computationally prohibitive within the present TDDFT framework, we instead use periodic arrays of inclusions as model systems.

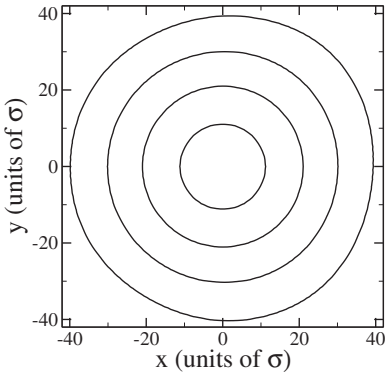

FIG. 4. Growth of HI-LM belonging to an array of period 160σ.

In a first series of simulations, we imposed conditions of growth in order to study the effect of increasing volume fraction. The evolution of the morphology of an inclusion so obtained is shown in Fig. 4; here, the period of the array is 160σ. The inclusion is found to remain essentially circular during growth, except near the end of the process where deformations develop, which are, however, quite small in comparison to those observed in the two-inclusion system (cf. Fig. 1). Constraints forced upon the inclusion by the complex environment therefore prove to be very strong, as expected.

While the impact of inclusion-inclusion interactions on morphology is relatively minor, the opposite is true for the chemical potential. The effect is in fact so strong that, as shown in Fig. 5, $\Delta\mu_i$ is completely dominated by elasticity by the time the volume fraction reaches about 5% (which occurs near $R_{eq}=15\sigma$ in the present geometry). Indeed, at

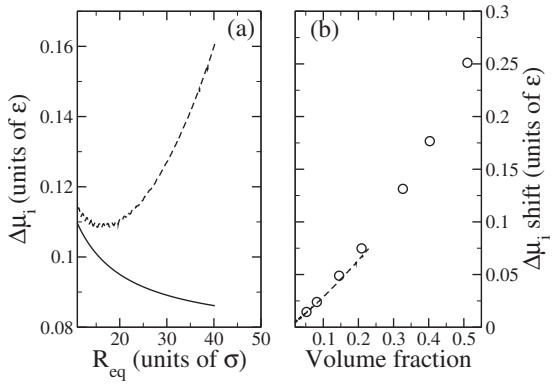

FIG. 5. Chemical potential difference $\Delta\mu_i$ (dashed lines) between species B and species A for an array of HI-LM of period 160σ. (a) $\Delta\mu_i$ as a function of size; the continuous line is for an isolated HI-LM and shows the normal capillarity-driven shift. (b) Shift in $\Delta\mu_i$ as a function of the volume fraction of the inclusions; the circles show the results for a periodic array of HI-LM following static relaxation; see text for details.

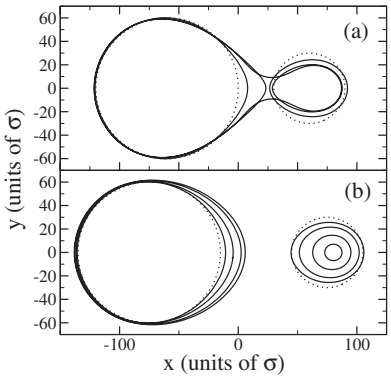

FIG. 6. Evolution in time of two SI-LM during coarsening: for interinclusion distance D=(a) 120σ and (b) 150σ.

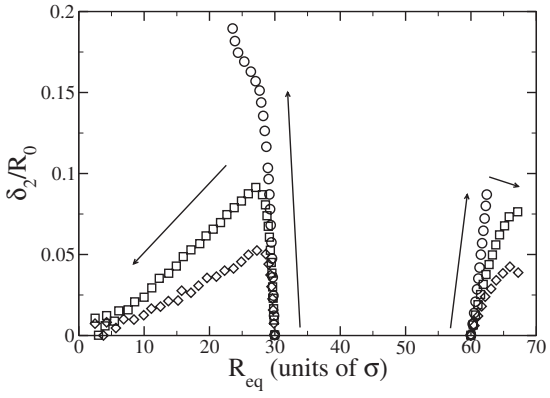

FIG. 7. Relative amplitude of mode 2 for different distances D between two SI-LM with initial radii of 30σ and 60σ, respectively: circles, $D=120\sigma$ [see Fig. 6(a)]; squares, $D=150\sigma$ [see Fig. 6(b)]; diamonds, $D=200\sigma$. Arrows indicate the flow of time.

this point, $\Delta\mu_i$ starts to *increase* with R_{eq}, while capillarity prescribes a $1/R_{eq}$ decay [continuous line in Fig. 5(a)]. Upon varying the separation D, we find that $\Delta\mu_i$ can be decomposed into the usual capillarity term plus a shift due to elastic interactions whose magnitude is controlled by the volume fraction; the latter is plotted in Fig. 5(b). The shift is initially a (roughly) linear function of the volume fraction. Note that a linear variation with volume fraction is equivalent to a D^{-2} dependence with respect to interinclusion distance, not too far from the $D^{-2.22}$ variation observed for pair interactions. However, as can be appreciated by comparing Figs. 5(b) and 3 (inset), typical shifts here are one or two orders of magnitude larger than in the two-inclusion system.

For high volume fractions, the above method cannot be used because the presence of a source of solute atoms close to the inclusion could lead to artificial effects. In this regime, we use instead a sequence of relaxations with periodic boundary conditions on the TDDFT equations, keeping the inclusion size fixed at $R=30\sigma$ and varying the size of the simulation cell. The results are presented as circles in Fig. 3(b). At low volume fraction, the measured shifts agree well with those obtained in the growth simulations, indicating that the elastic contribution indeed decouples from the capillarity contribution. At higher volume fraction, nonlinearities appear, further increasing the elastic shift. Note that for a volume fraction of 0.5, the shift amounts to ~300% of the value of $\Delta\mu_i$ for an isolated inclusion.

B. Interaction between soft inclusions

1. Two-inclusion systems

From Eshelby's formula, Eq. (1), we expect soft inclusions to exhibit a very different behavior than hard inclusions since the interaction is now attractive. Further, as shown by Johnson *et al.* [42], the local growth rate should be larger along the alignment axis than across, leading to the elongation of the inclusions along this axis. This is observed in our TDDFT simulations, as shown in Fig. 6. The inclusions gradually adopt an egglike shape, pointing toward one another, typical of interacting soft inclusions [44]. Our calculations reveal that shape changes occur rapidly for the small inclusion, but more slowly for the large one; also, as shown in Fig. 7, deformations occur at nearly constant size for the small inclusion, but develop concomitantly with growth for the large inclusion.

As coarsening proceeds, there are two possible outcomes: either the inclusions merge [see Fig. 6(a)] or the large inclusion grows at the expense of the small one [see Fig. 6(b)]. In the first situation, coalescence follows from the formation of a sharp tip on the inner surface of the large inclusion, which rapidly grows toward the small inclusion until the two merge. Soft inclusions are well known for their tendency to coalesce with their neighbors [19] and, as a result, the softer phase often assumes the role of the matrix, even at very low volume fraction [22]. This process is particularly efficient because a local elastic energy minimum (and hence a local chemical potential minimum) forms at sharp interface features such as tips [18]. Note that merging does not result from the displacement of the inclusions but, rather, from shape changes and directional growth. In the second situation, coarsening occurs diffusively: the small inclusion gradually evaporates and solute atoms diffuse toward the large one. In this process, the small inclusion returns to a circular shape while the large one becomes increasingly elliptic because of the anisotropic solute supply (see Fig. 7); the elongation is very large compared to the HI case. Only when the small inclusion has completely evaporated does relaxation toward a circular shape begin.

The lack of a significant spontaneous reorganization of the large inclusion in the present (soft) case, as compared to the hard case, can be explained by the relatively small amplitude of the elastic perturbations caused by the small inclusion (which has $k_{BB}=10\epsilon/\sigma^2$ vs $150\epsilon/\sigma^2$ for hard inclusions), while the capillary forces (which favor a circular shape) are roughly equal. The relatively small driving force pulling the large inclusion back to equilibrium can also be attributed to elasticity. Indeed, it is known that the elastic energy of an isolated soft inclusion is minimized for an ellipse instead of a circle, whereas the circle is preferred for a hard inclusion [46]. Thus, while both capillarity and elasticity favor the circle for hard inclusions, they compete in the case of soft inclusions, leading to a slower relaxation process. The formation of such long-lived, out-of-equilibrium shapes in growth conditions has been observed in our previous TDDFT calculation [18].

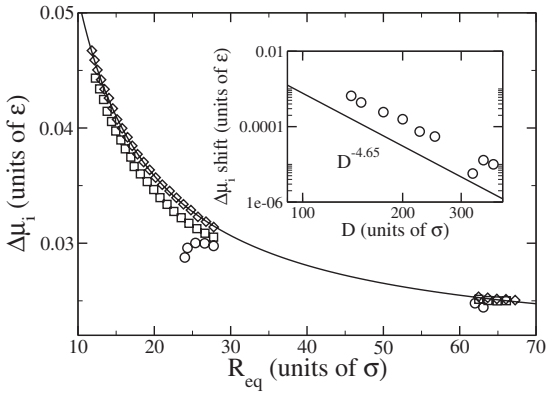

FIG. 8. Chemical potential difference $\Delta\mu_i$ between species B and species A as a function of size for two SI-LM with initial radii of 30σ and 60σ, respectively: circles, $D=120\sigma$; squares, $D=150\sigma$; diamonds, $D=300\sigma$; continuous line, $\Delta\mu_i$ for an isolated inclusion. Inset: shift in $\Delta\mu_i$ in the small inclusion as a function of D.

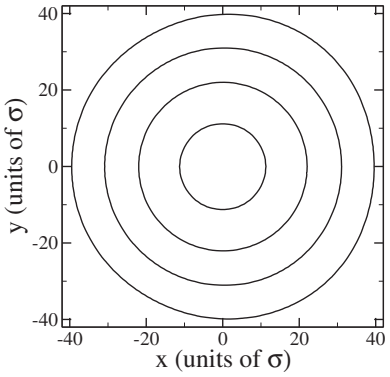

FIG. 9. Growth of SI-LM belonging to an array of period 160σ.

Even if the deformations of the two inclusions are now of comparable magnitude, the variations of the chemical potentials $\Delta\mu_i$ are still largely restricted to the small inclusion, as shown in Fig. 8. These results indicate that elastic corrections are very small for the large inclusion, even at small D. For the small inclusion, however, $\Delta\mu_i$ shifts slightly downward relative to the isolated inclusion (continuous line), in qualitative agreement with Eshelby's formula. As shown in the inset to Fig. 8, the magnitude of this shift decreases extremely rapidly with increasing distance, roughly as $D^{-4.65}$. It must be concluded that elastic interactions have a stabilizing effect only at very short separations, since the driving force for coarsening decreases with increasing interaction. Also, the shifts in $\Delta\mu_i$ are not primarily caused by changes in the shape of the inclusion but, rather, by the strain which is present within the inclusions.

For the parameters used here, inverse coarsening—which requires $\Delta\mu_i$ to be lower in the small inclusion than in the large one—is unlikely, as a very small size difference is required for the elastically induced shift to counterbalance the capillarity $1/R_{eq}$ term. But since the chemical potential shifts in the two inclusions have to be equal at equal sizes (by symmetry), the shift of the small inclusion decreases as its size increases relative to the large one. One can also obtain a sharp drop of $\Delta\mu_i$ in the smallest inclusion by decreasing D (circles in Fig. 8); this route, however, leads to coalescence, as we have seen above.

2. Periodic arrays of inclusions

We now turn to periodic systems of soft inclusions, first investigating the dependence on volume fraction; to this end, we impose growth on an array of inclusions with lattice constant fixed to 160σ. Here again, as shown in Fig. 9, the effect of interactions on the shape of the inclusions is very modest—compare to the two-inclusion system, Fig. 6. As in the case of hard inclusions, the presence of many neighboring inclusions efficiently impedes relaxation through shape changes.

Because of the limited efficiency of relaxation, the effect of interactions on the coarsening behavior increases considerably. Surprisingly, the sign of the chemical potential shift is also affected: as shown in Fig. 10, interactions now cause an increase of $\Delta\mu_i$ compared to isolated inclusions, even at small sizes (low volume fraction), while it was found to decrease in the two-inclusion system (see Fig. 8). Because of the lower elastic energies involved, the shifts in $\Delta\mu_i$ are however much more modest than for hard inclusions, reaching about 10% for a volume fraction of 0.35 [see Fig. 10(b)]. Further, the results at high volume fraction (obtained as discussed in Sec. IV A 2) indicate that the rate of increase of the shift decreases at higher volume fraction. Note, however, that the impact of interactions is still at least one order of magnitude larger in periodic systems than in two-inclusion systems. In the present case, these modest corrections are sufficient to counterbalance the $1/R_{eq}$ capillarity term for $R_{eq} > 50\sigma$ [the dashed line in Fig. 10(a) stops decreasing with increasing R_{eq}]. Finally, as is the case for hard inclusions, the shift in $\Delta\mu_i$ initially increases roughly linearly with volume fraction, indicating a D^{-2} dependence on interinclusion separation. This is much faster than the −4.65 exponent for the two-inclusion system, further demonstrating the efficiency of shape relaxation in limiting the effect of interactions on coarsening.

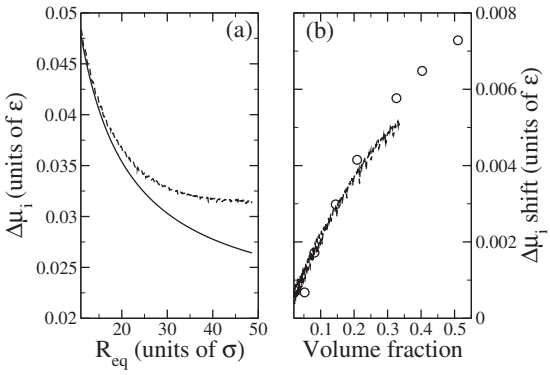

FIG. 10. Chemical potential difference $\Delta\mu_i$ (dashed lines) between species B and species A for an array of SI-LM of period 160σ. (a) $\Delta\mu_i$ as a function of size; the continuous line is for an isolated HI-LM. (b) Shift in $\Delta\mu_i$ as a function of the volume fraction of the inclusions; the circles show the results for a periodic array of SI-LM following static relaxation; see text for details.

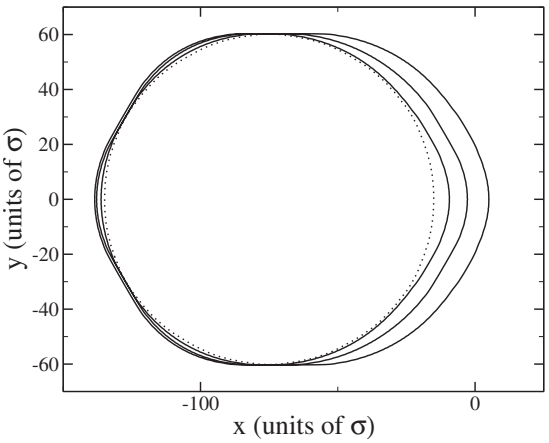

FIG. 11. Evolution in time of large SI-HM initially separated by $D=150\sigma$ from a small inclusion (located on the right; not shown) during coarsening. The dotted line represents the initial configuration.

C. The role of interface misfit

Having discussed the impact of bulk elasticity, we now turn to the specific role of interface misfits in systems of inclusions. This follows up on recent work where we demonstrated the importance of these misfits in the evolution of isolated inclusions in elastically inhomogeneous systems [25,26].

We examine first the impact of elastically induced kinetic faceting on coarsening. From a mesoscopic point of view, kinetic faceting results from the difference in growth speeds between different interfacial orientations [47]. During growth, the contribution of slow orientations (usually low-energy facets) to the shape of the inclusion increases, as fast orientations rapidly "grow out" of existence [48]. From a microscopic perspective, kinetic faceting occurs when the growth of preexisting terraces outpaces the nucleation of new terraces [49]. Conversely, upon evaporation, the slow orientations gradually disappear [48]. We have shown, using TD-DFT, that elasticity can intensify kinetic faceting through either the imposition of a barrier to the nucleation of new terraces, or the increase of the relative stability of steps compared to other sites at the surface [25,26].

An example of kinetic faceting is given in Fig. 11 for two SI-HM with $D=150\sigma$; only the large inclusion is displayed since kinetic faceting does not affect the small one (which lies on the right). The figure clearly shows the rapid formation of facets along the low-energy (10) orientations of the triangular lattice. Subsequent growth occurs by the successive addition of atomic layers on the facets facing the small inclusion; this gradually leads to the growth of the two facets parallel to the x axis, while other facets retain their original orientation and length. This behaviour is to be contrasted with that for the SI-LM case, Fig. 6(b), where the large inclusion adopts a smooth, facet-free shape which becomes increasingly elongated during growth.

Such morphological changes have consequences on the chemical potential of the inclusions; as shown in Fig. 12, $\Delta\mu_i$ actually increases in the large inclusion as growth proceeds, gradually pushing it away from the equilibrium curve.

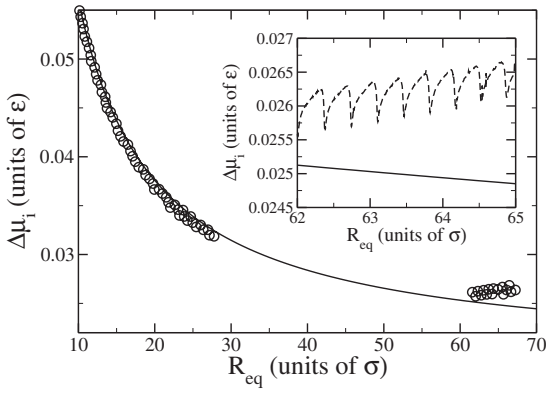

FIG. 12. Chemical potential difference $\Delta\mu_i$ between species B and species A as a function of size for two SI-HM with initial radii of 30σ and 60σ, respectively, $D=150\sigma$ apart. The inset is an enlarged view of $\Delta\mu_i$ for the large inclusion. The continuous lines give the behavior for an isolated inclusion.

This is to be contrasted with the low-misfit case (see Fig. 8), where kinetic faceting does not occur and the large inclusion closely follows the expected behavior. These results clearly demonstrate that, while $\Delta\mu_i$ is relatively unaffected by morphological modifications involving changes in the local curvature (see Sec. IV B), it is very sensitive to changes in the nature (i.e., rough vs faceted) of some regions of the interface. In contrast, the small inclusion remains free of facets and closely mimics the SI-LM behavior during coarsening.

Kinetic faceting affects coarsening because it allows inclusions to follow different $\Delta\mu_i(R_{\mathrm{eq}})$ curves upon growth or evaporation. In the present case, this results in a slowdown of coarsening since faceting of the large inclusion causes an increase of $\Delta\mu_i$ and hence a decrease in the driving force for diffusion. Notice that the magnitude of changes in $\Delta\mu_i$ due to kinetic faceting is relatively small compared to shifts due to elastic interactions in dense systems (see Fig. 10). Kinetic faceting could nevertheless become important in the later stages of coarsening when the size of the inclusions gets large (and hence the differences in $\Delta\mu_i$ get small) or when neighboring inclusions have similar sizes.

The importance of kinetic faceting in coarsening is, however, difficult to assess precisely because its occurrence makes the instantaneous state of inclusions history dependent. Indeed, partially faceted shapes can be very stable since large barriers may separate them from their equilibrium configuration [50]; the state of an inclusion at any given time is thus a function of the duration and intensity of previous growth and evaporation episodes. Adding to the difficulty is the fact that the faceting efficiency is strongly rate dependent. On the one hand, if growth is too slow, thermal fluctuations are able to restore the equilibrium shape of the inclusion—even in the presence of kinetic biases—and faceting will not occur. On the other hand, if growth is too fast, the differences in chemical potential between different atomic states of the interface become insignificant compared to the driving force so that kinetic roughening occurs instead [49]. Since the effects due to faceting are relatively small compared to those due to elasticity, we will not attempt to quantify further their impact.

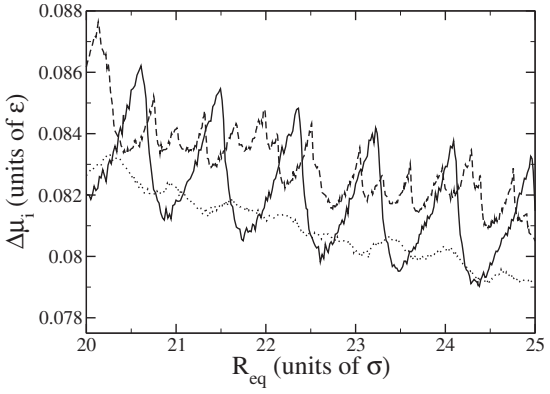

FIG. 13. Chemical potential difference $\Delta\mu_i$ between species B and species A as a function of size for two HI-HM with $D=150\sigma$ (dashed line), two HI-LM with $D=150\sigma$ (dotted line), and an isolated HI-HM (continuous line).

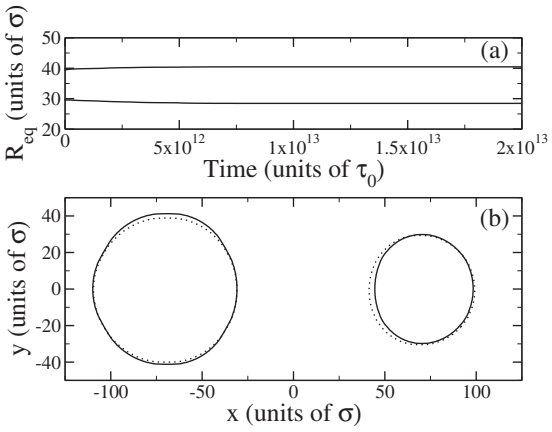

FIG. 14. Coarsening of two HI-HM with initial radii of 30σ and 40σ, respectively, separated by $D=140\sigma$: (a) time evolution of the equivalent radii of the inclusions; (b) initial (dotted lines) and metastable (continuous lines) shape of the inclusions.

The discrete nature of growth through successive additions of atomic layers also manifests itself in oscillations of $\Delta\mu_i$, as shown in the inset to Fig. 12 where maxima correspond to completely filled layers and minima to newly nucleated terraces. Oscillations occur because of modulations in the shape of the inclusions or changes in the energetics of interface sites available for addition (of solute atoms) or evaporation [26]. These oscillations are significant because they provide a pathway to the stabilization of microstructures. Indeed, oscillations act as chemical potential barriers hampering coarsening; while such barriers can be overcome by thermal fluctuations, they still slow down coarsening considerably by pushing the system away from a thermodynamically driven coarsening regime to a nucleation-driven regime [51].

Oscillations were observed in all the dilute elastically inhomogeneous systems we examined, and found to be strongest when the interface misfit is large [26]. Systems where interactions are important are no exception, as can be seen in Fig. 13. The oscillations in $\Delta\mu_i$ are in fact much larger for interacting HI-HM (dashed line) than for interacting HI-LM (dotted line). Comparison between the interacting HI-HM and the isolated HI-HM, however, indicates a significant decrease of the amplitude in presence of interactions. This can be explained by the reduced symmetry of the interacting system: because of the anisotropy of the strain field and of the supply of solute atoms, equivalent interfacial orientations in different regions of the inclusion grow at different speeds, leading to a desynchronization of the processes which cause oscillations in the chemical potential. In contrast, for a highly symmetric inclusion with an isotropic supply of solute atoms, these processes (e.g., the nucleation of new atomic layers) occur completely in phase. These arguments also explain the lack of regularity in the behavior of $\Delta\mu_i$ for interacting inclusions compared to the regular oscillations (of period $\sqrt{3}\sigma/2$—see Ref. [26]) for isolated inclusions. Note that when growth occurs in a layer-by-layer fashion, as is the case for the large SI-HM depicted in Fig. 11, oscillations can still be mostly regular, even in presence of interactions (see Fig. 12).

Despite their reduced amplitude, oscillations can still strongly hamper coarsening. Indeed, in a two-inclusion situation, if the intervals of $\Delta\mu_i$ swept the different inclusions overlap, i.e., $[\Delta\mu_i^{1,\min},\Delta\mu_i^{1,\max}]\cup[\Delta\mu_i^{2,\min},\Delta\mu_i^{2,\max}]\neq\emptyset$, a large number of metastable configurations become accessible. In contrast, in the purely capillarity-controlled case, the monotonic behavior of the chemical potential inexorably leads to a final state composed of a single inclusion. An example of such a metastable configuration is shown in Fig. 14 for a two-HI-HM system with initial sizes 40σ and 30σ: after a brief transient period, growth and evaporation cease and the configuration stabilizes. Such situations are extremely easy to obtain at high interface misfits: they appear as soon as the difference in $\Delta\mu_i$ between the inclusions and the amplitudes of the oscillations are comparable. Note that these configurations are not true equilibrium states because $\Delta\mu_i$ still decreases on average with increasing size (see Fig. 13). Thus, thermal fluctuations could overcome the chemical potential barrier imposed by oscillations, enabling coarsening to proceed further. However, since the chemical potential landscape is very rugged, a large number of crossings are required before the thermodynamic force can freely drive diffusion again. Short-period oscillations of the chemical potential thus provide a very robust mechanism leading to stabilization of microstructures, even in the presence of interactions.

V. DISCUSSION

A. Interactions and confinement

Our results emphasize the highly nonlinear character of elastic interactions between inclusions in multiphase alloys. Indeed, the response of an inclusion to the presence of a neighboring inclusion was found to depend strongly on the local environment or, more precisely, on the strength of constraints imposed by the local environment. If there is a single neighbor, for example, the constraints impeding elastic relaxation are small. In this case, as shown in Secs. IV A 1 and IV B 1, substantial shape changes take place and chemical potential shifts of at most a few percent (relative to isolated inclusions) can be expected, even for very small separations.

The calculated shifts are in qualitative agreement with the predictions of Eshelby's formula: interactions cause stabilization of soft inclusions and destabilization of hard inclusions. However, the magnitude of the corrections to the capillarity-driven behavior is so small that it is unlikely that coarsening could be significantly affected.

In the case where there are many neighboring inclusions, now, relaxation by shape changes becomes inefficient because of the severe constraints imposed by the environment. As discussed in Secs. IV A 2 and IV B 2, the effect on the chemical potential is one or two orders of magnitude larger than in the two-inclusion case. For both SI and HI, the interactions were found to *increase* the chemical potential, hence counteracting the normal $1/R_{eq}$ dependence of $\Delta\mu_i$. Further, the shifts were shown to be additive constants proportional to the volume fraction [see Figs. 5(b) and 10(b)].

These results suggest a simple model for the effect of interactions on the chemical potential shift of an inclusion, based on the following observation: neighboring inclusions may be viewed as obstacles impeding the relaxation of the internal strain energy of a given inclusion. Consider a single inclusion in an infinite two-dimensional matrix; the displacement field decays as $1/r$. Adding a second inclusion forces the displacement (or at least some of its components) to vanish somewhere along the line joining the two inclusions. Since there is still plenty of room in which to relax the excess elastic energy, shape changes are able to efficiently modify the strain field in order to make use of this free volume; impact on the chemical potential is therefore small. For a periodic array of inclusions, now, the displacement field is constrained in every direction, thus reducing considerably the volume available for the inclusion to relax its strain energy—here given by the volume of the unit cell of the array. In this case, a significant portion of the elastic energy remains stored within the inclusion, causing a strong increase of its chemical potential.

In order to test the validity of this simple model, we carried out a series of simulations where the volume available for the relaxation of the strain energy is efficiently controlled using finite-size cells rather than interactions between inclusions. To this end, zero-displacement boundary conditions were imposed on the elastic equilibrium equation while closed boundary conditions were used for the TDDFT equation. The simulation cell is either a regular hexagon with all sides varying between 40σ and 152σ, or a hexagon with four sides of length 72σ and two others of length varying between 40σ and 152σ. The angle between adjacent edges of the cells is set to $2\pi/3$. A single circular inclusion with $R_{eq}=30\sigma$ is placed at the center of each cell. The results of these calculations are reported in Fig. 15, together with those for a periodic array of inclusions (circles). From the finite-cell, regular-hexagon data (squares), we see that the effect of physically restricting the volume available for relaxation is indeed very similar to that resulting from the presence of other inclusions (circles). This agreement is not a fortuitous consequence of the high symmetry of the systems: for the irregular-hexagonal cells (diamonds), we find that inclusions are able to modify their shapes in order to make use of the strongly asymmetric distribution of free volume, similar to what is observed for two-inclusions systems. The end result

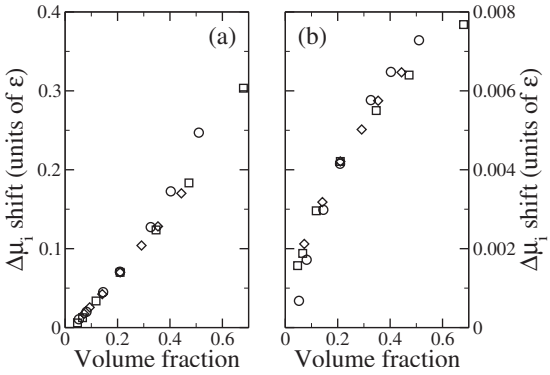

FIG. 15. Chemical potential shifts $\Delta\mu_i$ for (a) HI-LM and (b) SI-LM in different situations of confinement. Circles: periodic array of inclusions; squares, single inclusion in a regular-hexagon cell; diamonds, single inclusion in a hexagonal cell of varying aspect ratio (see text for details).

is then the same as if confinement were isotropic, as far as coarsening is concerned. Of course, it is not as easy to define the "volume available for relaxation" in nonsymmetric multi-inclusion systems; we will return to this important point below. While we are not interested in fixed-size systems *per se*, we will show below that the equivalence between different modes of confinement is useful for understanding the effect of interactions on coarsening.

This model helps understand why long-lasting inverse coarsening is usually not observed in simple microstructures composed of only a few inclusions. In such a case, confinement is poor since very large volumes are available to relax the elastic energy; elastic corrections are thus small and normal coarsening eventually prevails. In contrast, as the volume fraction increases, coarsening gradually shifts from "larger is more stable" to "larger volume available for relaxation is more stable" since elastic contributions to the chemical potential are proportional to the local volume fraction; this transition is clearly visible in Fig. 5, suggesting that inverse coarsening should be observed in a confined environment.

To test this hypothesis we studied the evolution of a two-HI-LM system in a hexagonal cell with two sides of length 256σ (along the axis joining the two inclusions) and four sides of length 128σ; we used closed boundary conditions for the TDDFT equations and zero-displacement boundary conditions for the elastic equilibrium equations. This finite cell emulates the confining effect of the environment. The initially circular inclusions had radii of 30σ and 40σ, respectively, and were 100σ apart, corresponding to an average volume fraction of ~ 0.1. The evolution of the system is presented in Fig. 16; as expected, the effect of confinement is strong: diffusion now carries solute atoms from the large to the small inclusion, i.e., inverse coarsening takes place. Diffusion, however, stops before the inclusions reach a common size, demonstrating the existence of other stable states besides the symmetric one. From Fig. 16(b), one also finds that, in contrast to the unconfined case, inclusions move during the simulation. Thus, under strong confinement, displacement of the inclusions and inverse coarsening are important for relaxing the strain energy; under weak confinement, this

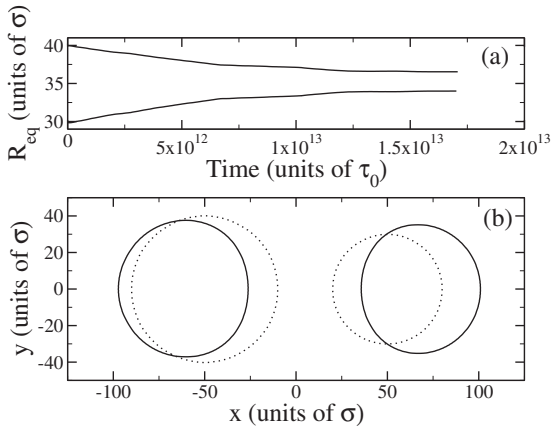

FIG. 16. Evolution of two HI-LM with initial radii of 30σ and 40σ, respectively, separated by $D=140\sigma$: (a) time evolution of the equivalent radii of the inclusions; (b) initial (dotted lines) and metastable (continuous lines) shape of the inclusions.

proceeds through shape changes alone. Note that inverse coarsening and motion of the inclusion are processes taking place on very long time scales $[(10^{12}-10^{13})\tau_0]$ compared to shape changes $(10^{11}\tau_0)$.

Inverse coarsening is found to be an extremely robust process in confined environments: in the system described above, it occurs for inclusions as small as 20σ; normal coarsening is restored only at smaller size. The final state, however, depends on the sizes of the inclusions and the distance between them, and both symmetric and asymmetric configurations are observed.

These results have important consequences regarding the volume available to each inclusion for relaxing its strain energy. In the system described above, the entire cell may be partitioned into two "available volumes," one for each inclusion. The occurrence of inverse coarsening implies that the effect of confinement is stronger on the large inclusion than on the small one or, equivalently, that in a multi-inclusion setting the volume available for the relaxation of an inclusion's strain energy scales sublinearly with its own volume. This is an extremely significant result since it implies that elasticity will eventually hamper the growth of larger-than-average inclusions.

B. Interactions and coarsening

We now investigate the consequences of these observations on the coarsening behavior of multi-inclusion systems. To this effect, we propose a simple LSW-type model modified to take the effect of elastic interactions into account; the LSW equations are solved numerically to yield the time evolution of the distribution in size of the inclusions. A similar model is described in detail in Ref. [26]. The only input needed is the relation between the activity (or, equivalently, $\Delta\mu_i$) and the size of an inclusion. The activity results from two contributions: one from capillarity, which decays as $1/R$, and one from elasticity, which we take to be linearly proportional to the local volume fraction, i.e., inversly proportional to the available volume (see Fig. 15):

$$\mathcal{A}_i(t) = C_1/R + C_2 V_f^l(R,t), \tag{3}$$

where C_1 is a parameter related to the interface free energy, C_2 describes the strength of elastic interactions, $V_f^l(R) = \pi R^2/V_i(R,t)$ is the local volume fraction around an inclusion of size R, related to the volume $V_i(R,t)$ available to an inclusion, which we assume proportional to its real volume to some power γ, $V_i(R,t)=N(t)(\pi R^2)^\gamma$, with $N(t)$ a time-dependent normalization factor ensuring that the sum of the V_i's is constant. As mentioned above, the existence of inverse coarsening in a confined geometry implies $\gamma<1$. In practice, the relation between the volume of an inclusion and the volume available to it for relaxation in a multi-inclusion setting is obtained by first calculating the chemical potential shifts for several nonsymmetric two-inclusion systems in confined geometry and then using the relation between chemical potential shift and available volume obtained from simulations of single inclusions in cells of fixed size. In this way, it is possible to parametrize the functional form proposed above; analysis of our simulation results indicates that $0.4<\gamma<0.6$. In what follows, we set $\gamma=0.5$. This choice, as well as the actual functional form used, is not critical, as we found no qualitative differences in the results for values of γ between 0 and 1. This is also true of the other parameters of the model, which affect only the length and time scales of the problem; we set $C_1=2.5\times10^{-4}\sigma^{-1}$ and $C_2=10^{-4}$.

Of course, this model can only give a rather crude description of the real coarsening dynamics. The LSW model is formally correct only in the limit $V_f\to0$. It is known that increasing the volume fraction leads to wider and more symmetric distribution functions than predicted by LSW, but that the coarsening exponent is not significantly altered [52]. Also, elastically induced correlations could modify the coarsening behavior; this possibility is not considered in LSW-type models because the inclusions are assumed to interact with the environment in a mean-field way. Thus, our model cannot be expected to yield quantitative results, but it should capture the essentials of elastic inhomogeneity.

The dependence on time of the average inclusion size $\langle R\rangle$ for different volume fractions V_f obtained within this model is presented in Fig. 17. We note first that in the dilute limit $(V_f\to0)$, coarsening is normal, well described by a single exponent $1/3$ as predicted by the LSW theory. In contrast, at finite volume fraction, significant departures from the normal behavior are observed, and coarsening is found to proceed in three distinct phases. First, after an initial transient period, a power-law dependence with an exponent somewhat smaller than $1/3$ is observed, and the higher the volume fraction, the smaller the exponent, which gradually decreases (intermediate phase), and finally reaches 0 (third phase)—the system stabilizes and coarsening apparently stops; this occurs at increasingly small average size as the volume fraction increases. Inverse coarsening sets in once $\langle R\rangle$ reaches its maximum value. This can indeed be seen from the size distribution function, shown in Fig. 18: at finite volume fraction (dashed line), the distribution gradually gets narrower (compare with the continuous curve for $V_f\to0$), converging to a δ function at later times. Such a behavior signals the

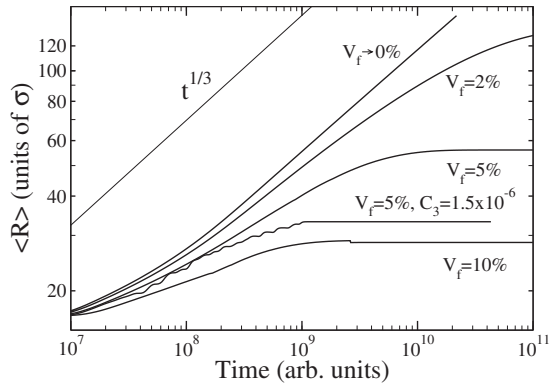

FIG. 17. Average inclusion size $\langle R\rangle$ for different volume fractions V_f obtained using a modified LSW model (see text for details); unless otherwise specified, $C_1=2.5\times10^{-4}\sigma^{-1}$, $C_2=1\times10^{-4}$, and $C_3=0$.

growth of small inclusions at the expense of larger ones, i.e., inverse coarsening.

In spite of its crude nature, our model is in remarkably good qualitative agreement with experiment. Stabilization has indeed been observed over long time scales in a wide range of inhomogeneous alloys [9,11,13]. Also, as expected, the maximum average size decreases with increasing volume fraction when stabilization occurs [9]. Finally, on small and intermediate time scales, a gradual decrease of the coarsening exponent with increasing volume fraction is observed, in agreement with experimental results [13]. Our simple model thus captures the essential physics of coarsening in elastically inhomogeneous systems.

Within LSW-type models, the existence of an asymptotic distribution function that is nonzero at a given finite R implies that the activity function possesses a minimum at this value of R. Indeed, any monotonically decreasing activity function leads to a distribution such that $\langle R\rangle\rightarrow\infty$. Elastic inhomogeneities yield such a minimum through the size-dependent chemical potential shifts which penalize large inclusions. While the narrowing of the distribution function observed in some alloys during the stable or very slowly coarsening stage [13] (third stage of the present model) is

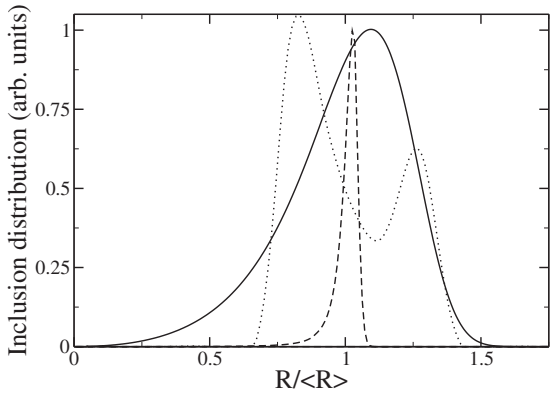

FIG. 18. Size distribution function for different values of the parameters of the modified LSW model, Eqs. (3) and (4). Continuous line, $\langle R\rangle=92\sigma$ with $V_f\rightarrow0\%$, $C_3=0$; dashed line, $\langle R\rangle=55\sigma$ with $V_f=5\%$, $C_3=0$; dotted line, $\langle R\rangle=33\sigma$ with $V_f=5\%$, $C_3=1.5\times10^{-6}$.

consistent with the presence of a single minimum, widening—also observed in some cases [11,12,16]—requires many. As demonstrated in Sec. IV C, chemical potential oscillations caused by interface misfits provide a mechanism for the existence of such a rugged landscape, enabling microstructures composed of inclusions of various sizes to become (meta)stable against coarsening. These oscillations can be accounted for by adding a term in Eq. (3), which we now write

$$\mathcal{A}_i(t)=C_1/R+C_2V_f^l(R,t)+C_3[\cos(4\pi R/\sqrt{3})+1]/2. \quad (4)$$

Since the results are not affected by the period of the oscillations we use, for simplicity, the value appropriate for isolated inclusions, viz., $\sqrt{3}/2\sigma$; we set $C_3=1.5\times10^{-6}$.

We previously demonstrated that oscillations alone, i.e., without elastic effects ($C_2=0$), are able to induce a transition from a normal coarsening state to a frozen state (with the present choice of parameters, this occurs at $\langle R\rangle\simeq140\sigma$ [26]) and that slowing down is accompanied by the formation of a long tail at large sizes in the distribution function. If contributions from both oscillations and elastic interactions ($C_2\neq0$, $C_3\neq0$) are included, now, the evolution of the microstructure is not modified dramatically. As shown in Fig. 17 for a volume fraction of 5%, the main differences are a decrease of the maximum $\langle R\rangle$, a slight decrease of the coarsening exponent in the first phase, and a reduction of the duration of the intermediate regime. In contrast, the size distribution is significantly affected. As illustrated in Fig. 18 (dotted line), it stabilizes with a finite width—wider than the normal LSW distribution—in agreement with the above discussion. Also, the formation of a long tail is avoided because elasticity prohibits the growth of very large inclusions. Note that, while widening is a robust feature of the model, the precise shape of the distribution function is quite sensitive to the amplitude of the oscillations.

These results demonstrate that the oscillations in the chemical potential induced by the interface misfits are able to stabilize microstructures containing inclusions of various sizes, even in presence of interactions. The oscillations are also able to prevent inverse coarsening and hence account for the widening of the distribution function observed in some alloys [11,16,12]. Finally, the model suggest that interface misfits strongly contribute to the slowing down of coarsening in cases where it initially occurs with an exponent close to 1/3 but then abruptly stops [9–11,13], since, as our model indicates, an exponent of 1/3 is associated with small bulk elastic effects. In this case, however, slowing down is expected to be very gradual (see Fig. 17 at low volume fraction); in contrast, the transition from normal coarsening to frozen state is possible in presence of large interface misfits [26]. In this case, bulk elasticity would only assist the transition by slowing down the growth of large inclusions, thus making the transition sharper. These results demonstrate that essentially all of the coarsening anomalies described above can be understood if the effect of both interactions and interfacial elasticity are considered.

As a final point, it must be mentioned that another mechanism besides oscillations may cause the stabilization of dis-

tribution functions of finite width: the ruggedness of the activity could indeed originate from local variations of the environment of the inclusions, an effect not taken into account in the present model. This would require some sort of self-organization of the available volumes, as simple random fluctuations eventually lead to a monodisperse distribution of inclusion sizes in absence of chemical potential oscillations. This problem will be the subject of further work. The fact that significant inverse coarsening was never observed in large-scale simulations [22,23,36] may indicate that such self-organization processes do occur. It may also be simply due to limitations in time of the simulations, as inverse coarsening only becomes significant in the very late stages of microstructural evolution, once the average inclusion size has reached its final value. Before this stage is reached, elasticity is only expected to slow down the growth of large inclusions in comparison to the homogeneous case.

VI. CONCLUSION

We have investigated the role of interactions between inclusions on the coarsening dynamics of elastically inhomogeneous alloys with lattice misfit. From our study of two-inclusion systems, we found that shape changes are the main process by which strain energy relaxes. The latter was found to be so efficient that coarsening is not significantly affected by interactions. However, we have also found that the efficiency of the mechanism drops for denser arrangements of inclusions, leading to corrections proportional to the local volume fraction. In this case, the effect of elasticity on coarsening increases by one or two orders of magnitude so that these corrections are sufficient to counteract the usual capillarity-dominated behavior. In contrast to what would be expected from Eshelby's formula, the effect of interactions is qualitatively the same if both hard and soft inclusions are organized in dense arrangements.

In the second part of this study, we examined the impact of interface elasticity on coarsening. Interactions were shown to modify very little the role of interface misfit in comparison to the dilute limit [26]: interface elasticity induces kinetic faceting or oscillations in the chemical potential of the inclusions. Both processes were shown to be able to significantly affect the coarsening behavior. In particular, oscillations were shown to stabilize microstructures containing inclusions of unequal sizes, without the need for some other stabilizing process like inverse coarsening. An example of an interface-stabilized system of inclusions was given.

In the last part, we showed that the effect of interactions on the chemical potential of inclusions is akin to the effect of confinement by cells of finite volumes. On the basis of this observation, we explained why dense arrangements of inclusions are required for inverse coarsening to take place; an example was presented. Finally, we proposed a modified LSW model to account for the effect of elasticity (both bulk and interface contributions) on coarsening. The predictions of the model were shown in Sec. V B to be in excellent agreement with the experimental observations: in bulk-elasticity-dominated systems, coarsening initially proceeds with a reduced exponent but gradually reaches a stable state through inverse coarsening; in interface-elasticity-dominated cases, transitions from a normal coarsening state with exponent $1/3$ to a stable state take place, and final inclusion distribution functions of finite widths are observed. The combination of these two effects is sufficient to explain essentially all the coarsening anomalies attributed to elastic effects.

This work demonstrates that elasticity provides two distinct pathways for controlling the morphology and coarsening kinetics of multiphase microstructures: the traditional route involving interinclusion interactions, and a novel route relying on interface effects. It should be possible to use this dichotomy to further enhance our control over microstructures. Indeed, on the one hand, interface elasticity provides an unselective stabilization process that can operate nearly irrespective of the morphological features of the microstructures. On the other hand, our results suggest that interinclusion interactions can only stabilize monodisperse microstructures; however, they can also induce shape changes and movement of inclusions. Careful balancing of these two factors could thus enable precise tuning of the microstructural properties, as hinted by the wide range of behaviors observed in real materials where these two factors simultaneously operate. However, understanding of the forces involved in microstructural evolution will not be complete until the impact of correlations between inclusions is understood: since both inverse coarsening and inclusion migration operate at high volume fraction, complex correlations, not taken into account here, could form and affect both kinetic and morphological features of the system. This will be the subject of future investigation.

ACKNOWLEDGMENTS

This work has been supported by grants from the Natural Sciences and Engineering Research Council of Canada (NSERC) and the Fonds Québécois de la Recherche sur la Nature et les Technologies (FQRNT). We are indebted to the Réseau Québécois de Calcul de Haute Performance (RQCHP) for generous allocations of computer resources.

[1] J. M. Garnett, Philos. Trans. R. Soc. London **203**, 385 (1904).
[2] S. Schmitt-Rink, D. Chemla, and D. Miller, Adv. Phys. **38**, 89 (1988).
[3] S. Torquato, S. Hyun, and A. Donev, Phys. Rev. Lett. **89**, 266601 (2002).
[4] A. C. Reddy and S. S. Rajan, Bull. Mater. Sci. **28**, 75 (2005).
[5] P. Merica, Trans. Am. Inst. Min., Metall. Pet. Eng. **99**, 13 (1932).
[6] I. Lifshitz and V. Slyozov, J. Phys. Chem. Solids **19**, 35 (1961).

[7] C. Wagner, Z. Elektrochem. **65**, 581 (1961).
[8] W. Ostwald, Z. Phys. Chem., Stoechiom. Verwandtschaftsl. **22**, 289 (1897).
[9] O. Paris, F. Langmayr, G. Vogl, and P. Fratzl, Z. Metallkd. **86**, 860 (1995).
[10] F. Langmayr, P. Fratzl, G. Vogl, and W. Miekeley, Phys. Rev. B **49**, 11759 (1994).
[11] A. Ges, O. Fornaro, and H. Palacio, J. Mater. Sci. **32**, 3687 (1997).
[12] H. Calderon, G. Kostorz, Y. Qu, H. Dorantes, J. Cruz, and J. Cabanas-Moreno, Mater. Sci. Eng., A **238**, 13 (1997).
[13] T. Miyazaki, in *Solid-Solid Phase Transformations*, edited by D. L. W. C. Johnson, J. M. Howe, and W. Soffa (Minerals, Metals and Materials Society, Warrendale, PA, 1994).
[14] A. Maheshwari and A. J. Ardell, Phys. Rev. Lett. **70**, 2305 (1993).
[15] Y. Yoo, D. Yoon, and M. Henry, Met. Mater. (Soeul, Rep. Korea) **1**, 47 (1995).
[16] H. J. Ryu, S. H. Hong, J. Weber, and J. H. Tundermann, J. Mater. Sci. **34**, 329 (1999).
[17] K. Thornton, N. Akaiwa, and P. W. Voorhees, Phys. Rev. Lett. **86**, 1259 (2001).
[18] D. Perez and L. J. Lewis, Phys. Rev. E **74**, 031609 (2006).
[19] P. Leo, J. Lowengrub, and H. Jou, Acta Mater. **46**, 2113 (1997).
[20] J. K. Lee, Mater. Sci. Eng., A **238**, 1 (1997).
[21] I. Schmidt, R. Mueller, and D. Gross, Mech. Mater. **30**, 181 (1998).
[22] J. Zhu, L. Chen, and J. Shen, Modell. Simul. Mater. Sci. Eng. **9**, 499 (2001).
[23] A. Onuki and A. Furukawa, Phys. Rev. Lett. **86**, 452 (2001).
[24] X. Li, K. Thornton, Q. Nie, P. Voorhees, and J. Lowengrub, Acta Mater. **52**, 5829 (2004).
[25] D. Perez and L. J. Lewis, Phys. Rev. Lett. **98**, 075501 (2007).
[26] D. Perez and L. J. Lewis, Phys. Rev. E **75**, 011604 (2006).
[27] J. D. Eshelby, Acta Metall. **14**, 1306 (1966).
[28] P. W. Voorhees and W. C. Johnson, Phys. Rev. Lett. **61**, 2225 (1988).
[29] C. Su and P. Voorhees, Acta Mater. **44**, 2001 (1996).
[30] W. C. Johnson, Acta Metall. **32**, 465 (1984).
[31] Y. Enomoto and K. Kawasaki, Acta Metall. **37**, 1399 (1989).
[32] A. Onuki and H. Nishimori, J. Phys. Soc. Jpn. **60**, 1 (1991).
[33] C. Su and P. Voorhees, Acta Mater. **44**, 1987 (1996).
[34] I. Schmidt, Comput. Mater. Sci. **22**, 333 (2001).
[35] S. Hu and L. Chen, Acta Mater. **49**, 1879 (2001).
[36] D. Orlikowski, C. Sagui, A. Somoza, and C. Roland, Phys. Rev. B **59**, 8646 (1999).
[37] D. Reinel and W. Dieterich, J. Chem. Phys. **104**, 5234 (1996).
[38] H. Fischer, J. Reinhard, W. Dieterich, J. Gouyet, P. Maass, A. Majhofer, and D. Reinel, J. Chem. Phys. **108**, 3028 (1998).
[39] M. Kessler, W. Dieterich, H. L. Frisch, J. F. Gouyet, and P. Maass, Phys. Rev. E **65**, 066112 (2002).
[40] E. B. Tadmor, R. Phillips, and M. Ortiz, Langmuir **12**, 4529 (1996).
[41] R. E. Miller and E. B. Tadmor, J. Comput.-Aided Mater. Des. **9**, 203 (2002).
[42] W. C. Johnson, P. W. Voorhees, and D. E. Zupon, Metall. Trans. A **20A**, 1175 (1989).
[43] A. Onuki and H. Nishimori, Phys. Rev. B **43**, 13649 (1991).
[44] H. Jou, P. Leo, and J. Lowengrub, J. Comput. Phys. **131**, 109 (1997).
[45] T. Abinandanan and W. Johnson, Acta Metall. Mater. **41**, 27 (1992).
[46] J. Eshelby, Proc. R. Soc. London, Ser. A **241**, 376 (1957).
[47] G. Wulff, Z. Kristallogr. **34**, 449 (1901).
[48] T. Uehara and R. Sekerka, J. Cryst. Growth **254**, 251 (2003).
[49] B. Mutaftschiev, *The Atomistic Nature of Crystal Growth*, Springer Series in Materials Science (Springer, Berlin, 2001).
[50] G. S. Rohrer, C. L. Rohrer, and W. Mullins, J. Am. Ceram. Soc. **84**, 2099 (2001).
[51] G. S. Rohrer, C. L. Rohrer, and W. Mullins, J. Am. Ceram. Soc. **85**, 675 (2002).
[52] P. W. Voorhees, J. Stat. Phys. **32**, 231 (1985).